Andre Webber
300286354

EEEN315 Project Report 1:

Open Loop Transfer Function for a Motorised Pendulum

Andre Webber-LaHatte

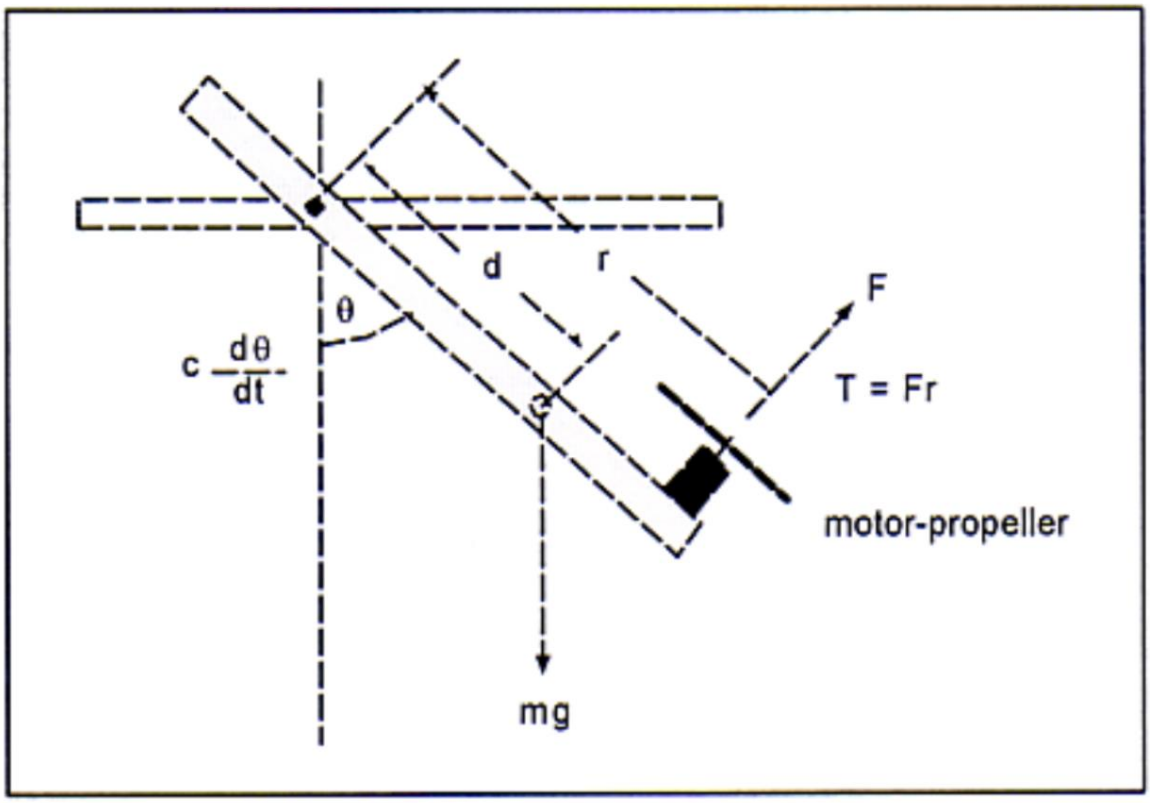

1. Introduction

Automated control of a process requires a system that behaves in a predictable, precise, and repeatable manner. To achieve this level of control, the behaviour of the system being controlled must be analysed and understood. How does the output of a system respond to a controlled input?

This report discusses, analyses, and defines the behaviour of a propeller driven pendulum to derive an open loop transfer function. Through systems identification and analysis of measurement data I found the 4th order transfer function that relates the voltage applied at the propeller motor, to the angular displacement of the pendulum. A key observation is that the pendulum has a much greater impact on the behaviour of this system compared with the propeller. Carrying out this exercise has allowed me to gain insight into a way of thinking required for systems identification, clarified misconceptions I had about the operation of brushed DC motors, and reinforced theory being taught in EEEN315 lectures.

2. Method

Controlling the angle of a propeller driven pendulum requires finding a transfer function that relates a voltage input to an angular displacement output. Derivation of the transfer function was done by breaking the entire system down into multiple subsystems, and finding the transfer function for each subsystem. Figure 1 is a basic digram for a propeller driven pendulum, showing how a torque input relates to an angular displacement output. The entire system can be broken down as follows. A voltage input drives the propeller motor to some angular velocity. The angular velocity of the propeller results in a thrust, or force, normal to its rotational plane. The thrust produced by the rotation of the propeller results in a torque on the pendulum which causes it to swing up to, and settle on some angle. Figure 2 is a block digram that breaks the system down into the sub systems described. K_p is the ratio between the propeller speed and the thrust, and r is as labelled in figure 1.

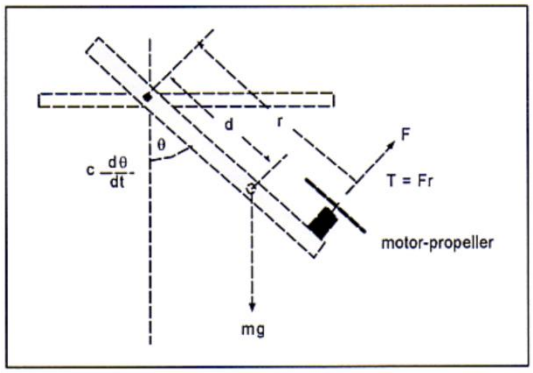

Figure 1: Diagram for a propeller driven pendulum.

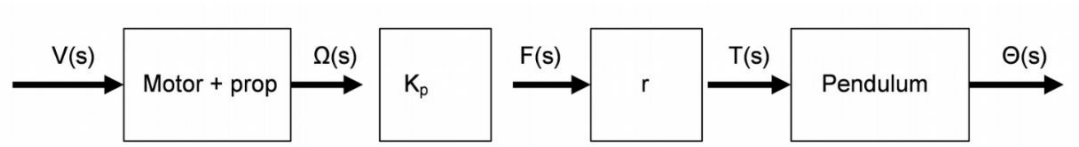

Figure 2: Block diagram showing the subsystems in a propeller driven pendulum.

2.1 The Motor

The propeller is driven by a brushed DC motor. The motor consists of a permanent magnet stator and a shaft that carries an armature coil [1]. Voltage is applied to the armature coil through a connection between brushes and a commutator. A current though the armature generates a magnetic field which interacts with the stator field resulting in a torque on the shaft. As the shaft rotates, the commutator makes and breaks the connection with the

brushes to reverse the direction of the current. An electromotive force (emf) is generated on the armature as it moves through the stator field.

The motor and propeller system needed to be broken down further to find a transfer function relating voltage to motor speed. The subsystems identified are the electrical, and mechanical systems [1]. The electrical system has a voltage input that determines the armature current. The mechanical system has a torque input, proportional to the armature current, and determines the angular velocity of the motor shaft. The emf induced on the armature (back emf) works as negative feedback proportional to the motor speed. Figure 3 shows a block digram for the motor with each of these subsystems.

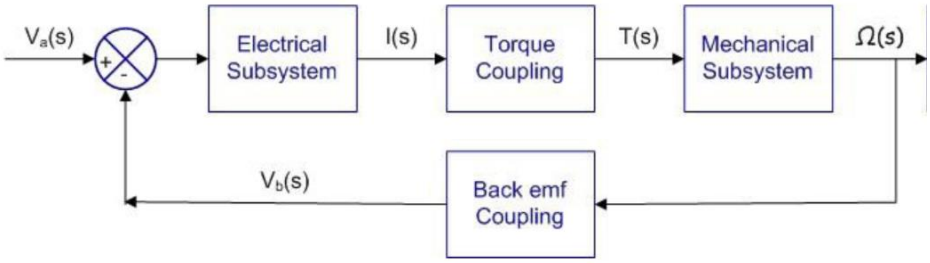

Figure 3: Block digram showing the subsystems in a brushed DC motor.

Figure 4 shows an equivalent circuit for a brushed DC motor. $v_a(t)$ is the armature voltage, $i_a(t)$ the armature current, R_a and L_a represent the resistance and inductance of the armature winding, and $e(t)$ ($v_b(t)$ from here on) is the back emf. A Differential equation relating i_a to $v_a - v_b$ can be formed using Kirchoff's voltage law, see Eq. (1). Equation (2) shows the Laplace transform of Eq. (1), leading to Eq. (3), the transfer function for the electrical subsystem.

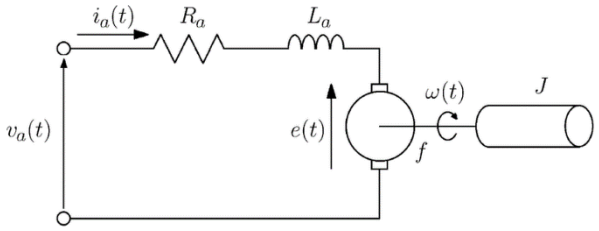

Figure 4: Equivalent circuit of a brushed DC motor [2].

$$L_a \frac{di}{dt} + R_a i(t) = v_a(t) - v_b(t) \quad (1)$$

$$L_a s I(s) - R_a I(s) = V_a(s) - V_b(s) \quad (2)$$

$$\frac{I(s)}{V_a(s) - V_b(s)} = \frac{1}{L_a s - R_a} \quad (3)$$

The torque applied to the motor shaft is proportional to the armature current, as shown in Eq. (4). Figure 5 shows a basic digram for a motor shaft, with the assumption the shaft angle is changing in the same direction as the applied torque. The net torque on a rotating body is equal to the load inertia, J_m, multiplied by the angular acceleration, and the damping is proportional to the angular velocity by D_m. Using $\omega(t)$ to represent angular velocity, the net torque and damped torque form the differential equation in Eq. (5). Equation (6) shows the Laplace transform of Eq. (5), and Eq. (7) is the transfer function for the mechanical subsystem. The back emf is proportional to the angular velocity, shown in Eq. (8).

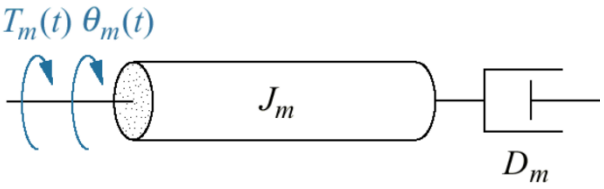

Figure 5: Diagram of torque being applied to a motor shaft [1].

$$\frac{T(s)}{I(s)} = k_T \tag{4}$$

$$J_m \frac{d\omega}{dt} + D_m \omega(t) = T_m(t) \tag{5}$$

$$J_m s\Omega(s) + D_m \Omega(s) = T(s) \tag{6}$$

$$\frac{\Omega(s)}{T(s)} = \frac{1}{J_m s + D_m} \tag{7}$$

$$\frac{V_b(s)}{\Omega(s)} = k_b \tag{8}$$

Figure 6 shows the block diagram for the motor, with each block replaced by its transfer function. By using the formula in Eq. (9), the various transfer functions that make up the motor can be combined into a single transfer function. Equation (10) shows the forward gain, the loop gain can be seen in Eq. (11), and the transfer function for the entire motor block in Eq. (12).

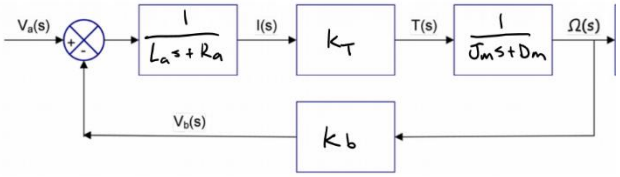

Figure 6: Motor block diagram with transfer functions.

$$\frac{\Omega(s)}{V_a(s)} = \frac{forward\ gain}{1 + loop\ gain} \tag{9}$$

$$forward\ gain\ = \frac{k_T}{(L_a s + R_a)(J_m s + D_m)}$$

(10)

$$loop\ gain = \frac{k_T k_b}{(L_a s + R_a)(J_m s + D_m)}$$

(11)

$$\frac{\Omega(s)}{V_a(s)} = \frac{\frac{k_T}{J_m L_a}}{s^2 + \frac{J_m R_a + D_m L_a}{J_m L_a} s + \frac{R_a D_m + k_T k_b}{J_m L_a}}$$

(12)

Ordinarily the values for $R_a, L_a, k_T, J_m, D_m,$ and k_B would be measured by analysing the motor in a lab, however due to public health measures taken during a global pandemic, these values were provided from measurements taken in previous years. Simulation of this transfer function with known values is discussed in section 3.

2.2 The Pendulum

To relate a torque input to an angular displacement output, the pendulum does not need to be broken down into further subsystems. Like the motor shaft, the net torque on the pendulum is the product of its inertia and angular acceleration. Where the motor shaft typically has its centre of gravity at its pivot point, figure 1 shows that the pendulum's centre of gravity as at some distance, d, from the pivot point. The positional difference between the pivot point and centre of gravity means that gravity will apply torque on the pendulum proportional to the sine of its angle. With J_P as the pendulum inertia, c the damping coefficient, m the mass of then pendulum, and g the gravitational constant, Eq. (13) shows a differential equation relating applied torque to angular displacement.

$$J_P \frac{d^2\theta}{dt^2} + c\frac{d\theta}{dt} + mgd\sin\big(\theta(t)\big) = T(t)$$

(13)

The non-linearity of gravitational torque with angular displacement makes this system difficult to transform into the Laplace domain. This non-linearity can be dealt with using small angle approximation. Figure 7 shows the difference between θ and $\sin\theta$ from 0 to $\frac{\pi}{4}$ radians (0° to 45°). For small angles (in radians) $\sin\theta \approx \theta$. This small angle approximation begins to diverge at around 0.35 radians (~20°), however may be suitable for larger angles up to 0.5 radians (~28.65°). The differential equation in Eq. (13) can be re-written as in Eq. (14). With gravitation torque linear in angle, Eq. (14) can be used to form the transfer function, Eq. (15).

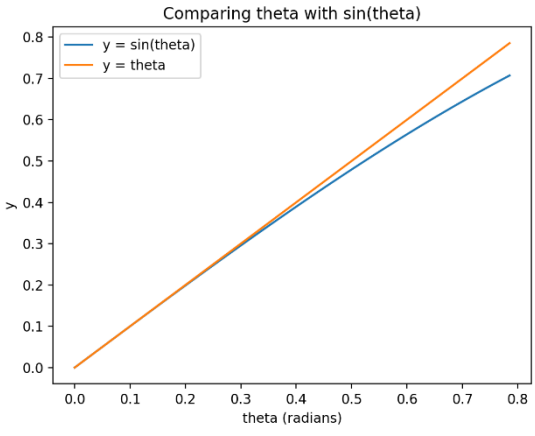

Figure 7: The small angle relationship between ϑ and $\sin\vartheta$.

$$J_P \frac{d^2\theta}{dt^2} + c\frac{d\theta}{dt} + mgd\theta(t) = T(t)$$

(14)

$$\frac{\Theta(s)}{T(s)} = \frac{1}{J_p s^2 + cs + mgd}$$

(15)

To find the coefficients J_p and c we were provided data from measurements taken in previous years. By moving the undriven pendulum to some angular displacement, letting it go, and allowing it to oscillate until it settles on 0 radians, the angle can be measured at regular time intervals to obtain data for angular displacement vs time. Angles were measured by sampling the voltage output from a potentiometer whose position is controlled by the angle of the pendulum. Figure 8 shows a plot of this data, it is uncertain what unit is used for angular displacement in this data as the initial value is -255. Values J_p and c can be estimated by using Eq. (16), the mathematical model for an undriven, damped oscillator responding to a disturbance [4], as well as Eq. (17) which relates the frequency of oscillation to the inertia and damping coefficient of the pendulum.

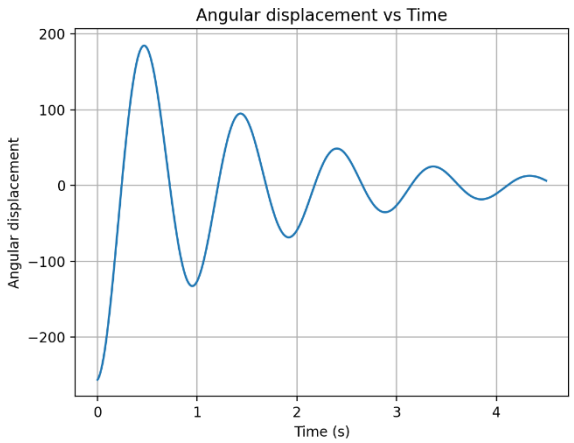

Figure 8: Graph of angle vs time for the undriven pendulum

$$y(t) = Ae^{-\frac{c}{2J_P}t}\cos(\omega_d t + \phi)$$

(16)

$$\omega_d = \sqrt{\frac{mgd}{J_P} - \left(\frac{c}{2J_P}\right)^2}$$

(17)

ω_d can be found by dividing 2π by the average time between each peak to obtain a frequency in $rads^{-1}$. Figure 8 shows an initial value of -255, and the oscillations appear to be settling on 0, by dividing the first peak by 255, the overshoot, M_P, can be estimated which can be used to determine the value of $\frac{c}{2J_P}$ with the equations bellow.

$$\zeta = \frac{-\ln M_P}{\sqrt{\pi^2 - \ln^2 M_P}}$$

(18)

$$\theta_P = \cos^{-1}\zeta$$

(19)

$$\omega_n = \frac{\omega_d}{\sin\theta_P}$$

(20)

$$\zeta\omega_n = \frac{c}{2J_P}$$

(21)

Equation (18) shows the damping ratio as a function of overshoot, Eq. (19) obtains the complex pole angle from the damping ratio, Eq. (20) obtains the natural oscillating frequency, and Eq. (21) gives the decay rate ($\frac{c}{2J_P}$) for Eq. (16). Once the value for $\frac{c}{2J_P}$ is known, the value for J_P can be found using Eq. (17), after which c can be found using Eq. (21).

2.3 Combining the Blocks

Figure 2 shows 2 blocks between the motor subsystem and the pendulum subsystem. The first of these 2 blocks is a linear function relating propeller speed to thrust. The value K_P has been provided from previous years data. The second of the 2 blocks relates the force generated by the propeller to the torque on the pendulum, this is a linear relationship with the coefficient being the distance from the pendulum pivot point to the centre of the propeller, or r is in figure 1.

As this is an open loop system, the transfer function giving angular displacement output from a voltage input can be found by multiplying each block. That is, multiply Eq. (12) and Eq. (15) with the coefficients K_P and r. Eq. (22) gives the transfer function for the entire system.

$$\frac{\Theta(s)}{V(s)} = \frac{\frac{k_T K_P r}{J_m L_a}}{J_P s^4 + \left(c + \frac{J_P(J_m R_a + D_m L_a)}{J_m L_a}\right)s^3 + \left(mgd + \frac{c(J_m R_a + D_m L_a) + J_P(R_a D_m + k_T k_B)}{J_m L_a}\right)s^2 + \left(\frac{mgd(J_m R_a + D_m L_a) + c(R_a D_m + k_T k_B)}{J_m L_a}\right)s + \frac{mgd(R_a D_m + k_T k_b)}{J_m L_a}}$$

(22)

3. Results

Values given for $R_a, L_a, k_T, J_m, D_m,$ and k_B were given as follows; $R_a = 6.3\Omega$, $L_a = 797mH$, $k_b = 0.0043\frac{Vs}{rad}$, $k_T = 0.0043\frac{Nm}{A}$, $D_m = 5.53 \times 10^{-6}\frac{Nms}{rad}$, and $J_m = 2.41 \times 10^{-6} kgm^2$. Using these values and the transfer function in Eq. (12), this gives the motor being used a transfer function as in Eq. (23). Figure 9 shows the response of this system for different sized step inputs.

$$\frac{\Omega(s)}{V(s)} = \frac{2238.7}{s^2 + 10.1992s + 27.7644}$$

(23)

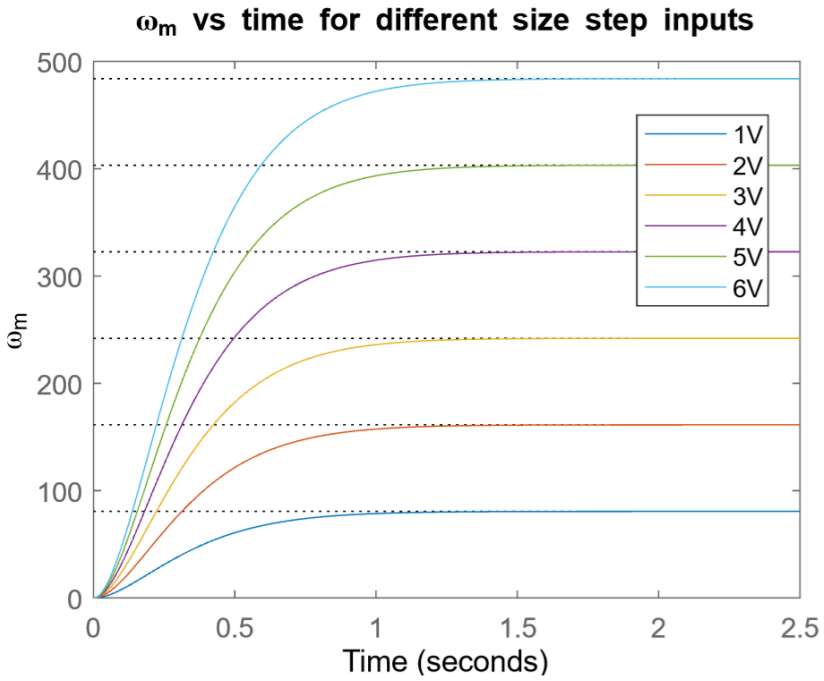

Figure 9: Motor speed responses to different sized voltage step inputs

Using the method described in section 2.2, I obtained the following values for the pendulum subsystem; $\omega_d = 6.5 rads^{-1}$, $\frac{c}{2J_P} = \sigma = 0.6689$, $J_P = 0.0054$, and $c = 0.0072$. The mass and distance to the pendulum's centre of gravity are given as; $d = 0.14m$, and $m = 0.168kg$. Using these values with the decaying oscillation in Eq. (16), and the transfer function in Eq. (15), I obtained Eq. (24) and Eq. (25). Figure 10 shows Eq. (24) plotted on top of the data provided for angular displacement vs time. Figure 11 shows a pole-zero map for the transfer function in Eq. (25). Figure 12 shows the step response for the pendulum subsystem.

$$\theta_{data}(t) = -255e^{-0.6698t}\cos(6.5t) \tag{24}$$

$$\frac{\Theta(s)}{T(s)} = \frac{1}{0.0054s^2 + 0.0072s + 0.2307} \tag{25}$$

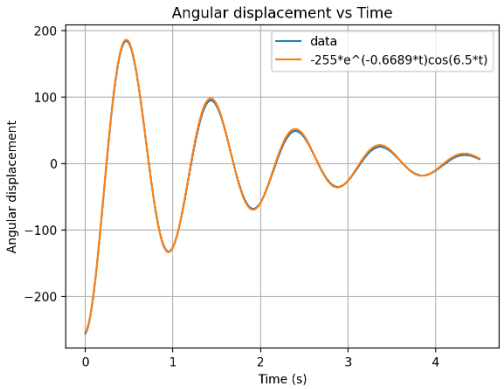

Figure 11: Eq. (24) plotted on top of provided data.

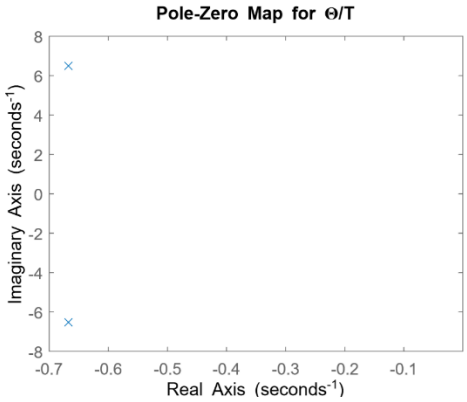

Figure 10: Pole-Zero Map for $\frac{\Theta(s)}{T(s)}$

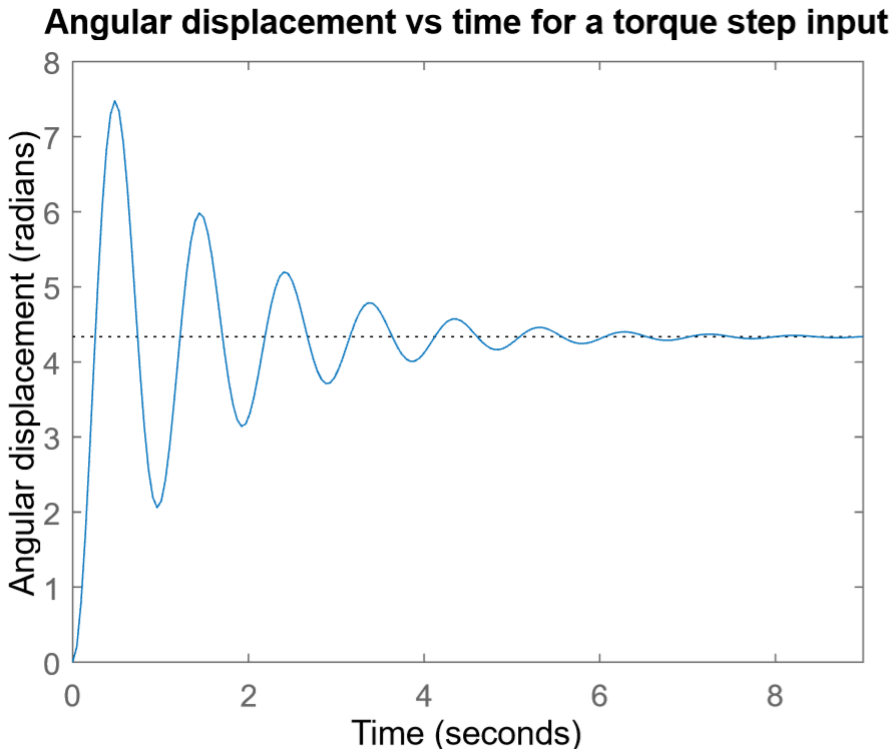

Figure 12: Step response for pendulum subsystem.

The value K_P was obtained from previous years data. This was done by placing the propeller on a scale and looking at how much the scale reading changed as the propeller speed was increased. The value provided gave $K_P \approx 0.0053$, the value for r as in figure 1 was given as $r = 0.165m$. Combining the blocks in figure 2 with known values givens the transfer function as in Eq. (26). Figure 13 shows a pole-zero map for the transfer function in Eq. (26), and figure 14 shows the response of the entire system to difference sized voltage step inputs.

$$\frac{\Theta(s)}{V(s)} = \frac{1.9577}{0.0054s^4 + 0.0623s^3 + 0.4541s^2 + 2.5529s + 6.4052}$$

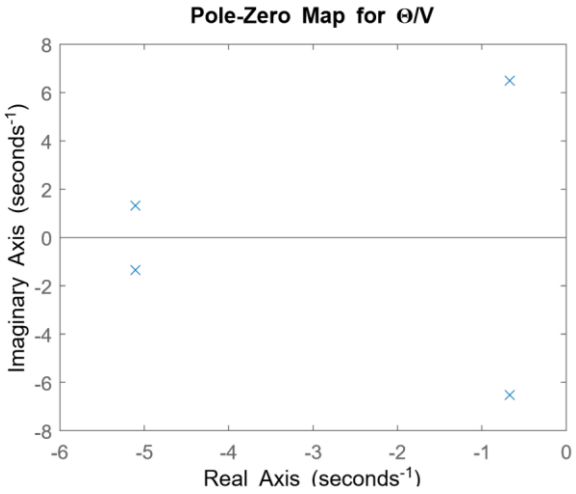

Figure 13: Pole-Zero Map for $\frac{\Theta(s)}{V(s)}$

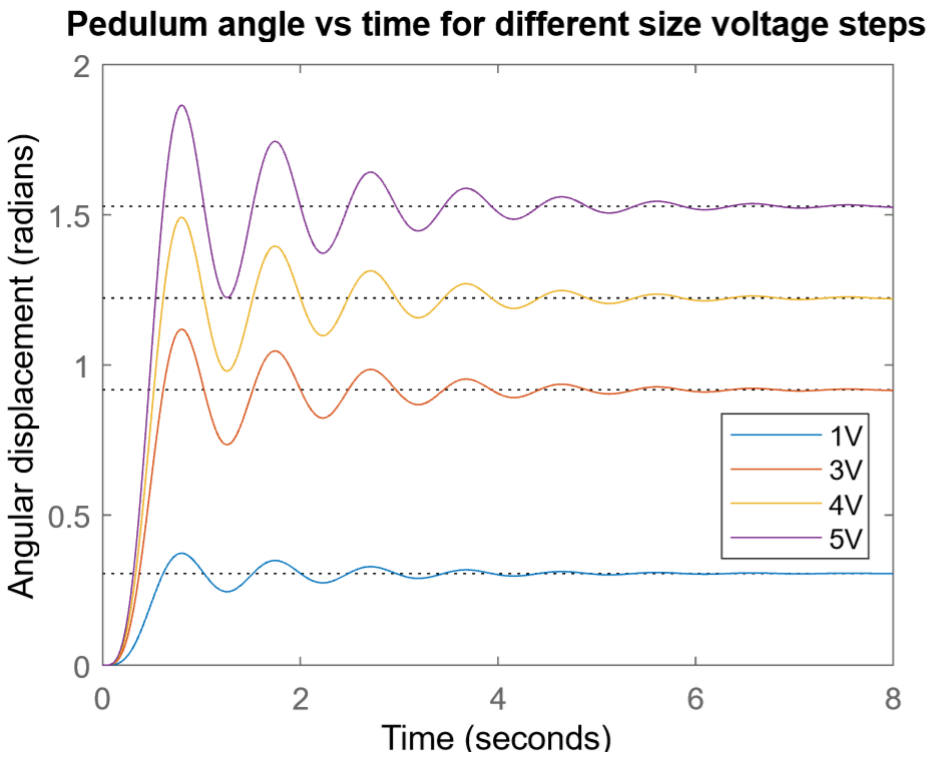

Figure 14: Response of entire system to different size step inputs.

4. Discussion

Completing this excercise through simulation has been useful in reinforcing the theory being taught in lectures. Derivation of the motor transfer function has helped to demonstrate a thinking style that is needed for breaking down a system into subsystems, particularly with identifying feedback that exists within a system. Analysing the data given for a step input to the undriven pendulum has given a chance to apply techniques taught in class, and better appreciate them. The process of completing this exercise has helped me to develop skills and insight in systems identification and how to model a system with a differential equation.

Most students presently at my level of education have had the entirety of their degree disrupted by a pandemic. One major disruption is a result of physical distancing requirements restricting lab access. While useful for time management, the lack of physical measurement taken in this project due to the pandemic has neglected what seems to be an important part of this process. Having had to deal with similar decisions made in previous papers has created a gap in knowledge relating to measurement and error analysis through lack of experience. I feel that it may have been more useful to scale back, but not completely remove the physical measurement aspect of this project to provide an opportunity that may help close a developing gap in knowledge.

Observing the results of simulating the transfer function for the motor presented something seemingly counterintuitive. See in figure 9 that the steady state gain of the motor remains consistent at $\sim 80.63 \frac{rad}{Vs}$ for varying sized step inputs. The proportional relationship between motor speed and back emf suggests that the impact of increases in armature voltage to motor speed will decrease as the voltage gets greater. The results in figure 9 show this not to be the case and have thus given me insight regarding the impact of back emf to

the ratio between armature voltage and motor speed. Considering the linear relationship between current and torque, then torque and speed, doubling the speed requires doubling the current. Given steady state current is given by $\frac{v_a - v_b}{R_a}$, with some initial current $i_{a_1} = \frac{v_{a_1} - v_{b_1}}{R_a}$, to double the speed $i_{a_2} = 2i_{a_1} = \frac{2(v_{a_1} - v_{b_1})}{R_a} = \frac{v_{a_2} - v_{b_2}}{R_a}$, because the motor speed has doubled $v_{b_2} = 2v_{b_1}$, therefore it must be that to double the motor speed $v_{a_2} = 2v_{a_1}$. In all, the steady state gain for a brushed DC motor is independent of input voltage (assuming the motor has not reached saturation).

Analysis of how the pendulum behaves to torque inputs gave the largest opportunity to apply theory taught in class. Rather than looking at the amplitude decay and curve fitting as suggested, I chose a different approach as outlined in section 2.2. The results speak for themselves, see in figure 11 how closely the model obtained from analysis matches the plot of the test data. I will note that in figure 12 that the steady state angle from a step input is far beyond the point where the small angle approximation shown in figure 7 starts to diverge form the true value, and in fact shows that it will settle on an angle $> 180°$. It is reasonable to assume that this system is not appropriate for torques $\geq 1Nm$, and that appropriate applied torque may be much smaller than $1Nm$.

The results of this exercise have shown that the angular displacement of a propeller driven pendulum given a voltage input can be modelled with a 4th order transfer function. Figure 13 shows that the poles contributed by the pendulum transfer function (Eq. (25)) will dominate and the system will behave similarly to steps in voltage as it would to steps in torque alone. Observe in figure 14 that for a step of 1V, the settled angle is near the point where the small angle approximation (see figure 7) starts to diverge. I would expect this system would work with steady state voltage inputs between 1 and 2V.

5. Conclusion

Observing the behaviours of a propeller driven pendulum has resulting in derivation of the open loop transfer function of the system. This is a 4th order transfer function that will be dominated by the decaying oscillation of the pendulum, so slight variations in the behaviour of the DC motor will have little impact on the system. Given the divergence in small angle approximation at $\sim 0.35 radians$, appropriate input voltages for steady state will be between 1 and 2V.

The process of modelling the behaviours of a propeller driven pendulum has given me insight into control systems engineering, as well as the operation of certain electrical components. Breaking down this system into subsystems, then further subsystems has introduced me to a way of thinking that will help develop my skills in systems identification. The application of analytical techniques when observing the behaviour of the undriven pendulum has reinforced theory taught in lectures.

References

[1] Understanding small, brushed DC motors, G.J. Gouws, August 2008

[2] J. C. Basilio and M. V. Moreira, "State-space parameter identification in a second control laboratory," in IEEE Transactions on Education, vol. 47, no. 2, pp. 204-210, May 2004, doi: 10.1109/TE.2004.824846.

[3] Control of a motorised pendulum, Lab 3: Transfer function of the pendulum and testing system open loop response, D Burmester, March 2022